

Development of a Vibration Device for Grinding with Microvibration

Z. W. Zhong* and H. B. Yang

School of Mechanical and Production Engineering, Nanyang Technological
University, Singapore, Republic of Singapore

ABSTRACT

This study aimed to develop a device to facilitate grinding experiments with microvibration for analyzing the vibration effect on surface finish of ground surfaces. A microvibration device was designed and fabricated. It can be used to provide microvibration to the workpiece vertically and/or horizontally during grinding. The relationship of the driving voltage, vibration displacement, and frequency was established. The vibration displacement of the device developed is proportional to the driving voltage amplitude for both vibration directions. The vibration frequency and displacement can be adjusted during the grinding process. Grinding experiments were carried out to compare the surface finish of silicon samples ground with and without microvibration. The results verified that microvibration of the workpiece along a certain direction during grinding can affect the surface finish of the ground workpiece.

Key Words: Design; Vibration device; Microvibration; Displacement; Frequency; Experiments; Grinding; Silicon; Surface roughness; Piezoelectric actuators; Power amplifier; Bandwidth; Cross-feed direction; Vertical direction; Table-feed direction.

*Correspondence: Z. W. Zhong, Ph.D., School of Mechanical and Production Engineering, Nanyang Technological University, 50 Nanyang Ave., Singapore 639798, Republic of Singapore; Fax: 65-6791-1859; E-mail: mzwzhong@ntu.edu.sg.

1. INTRODUCTION

Grinding is often used after production of materials and products. The grinding force level determines how fast the material removal rates are, how rough the remaining surface is, and whether the workpiece is metallurgically damaged.^[1–5] Grinding is a major manufacturing process that accounts for about 20 to 25% of the total production cost of machining of components.^[6] Therefore, many manufacturing companies have a growing interest in finding economical ways of improving grinding productivity in terms of part quality and production cost.

Grinding of aspherical surfaces made of Si and SiC was carried out by using diamond grinding wheels.^[7,8] Mirrors were successfully obtained by automatic grinding operations with mirror surface finish. Microphotographs demonstrated the ductile mode in grinding of silicon. Ground silicon carbide had complete ductile mode surfaces. By using a new device for dressing of a resin-bonded diamond wheel and an improved coolant system, ductile mode grinding of silicon and glass was achieved using an inexpensive, conventional surface grinding machine.^[9] Silicon samples were ground along different crystallographic directions under the same experimental conditions. R_a and R_q values and microphotographs of ground silicon surfaces showed the dependency of surface finish on the grinding direction.^[10]

Previous work on vibration-assisted machining shows that a number of process parameters can be influenced. Ductile cutting of soda-lime glass was realized by grooving experiments and applying ultrasonic vibration to a single-crystal diamond tool in the cutting direction. The critical depth of cut in grooving was increased to about seven times of that for conventional cutting. Better machining performance and reduction of tool wear were achieved. A transparent surface of soda-lime glass was obtained by ultrasonic vibration cutting. An optical quality surface ($R_{\max} = 0.03 \mu\text{m}$) was obtained.^[11]

Ultraprecision diamond machining of steel, which was generally considered impossible, was realized by applying ultrasonic vibration. High-quality surfaces with roughness less than $0.1 \mu\text{m}$ in R_{\max} were obtained stably up to a cutting distance of 1600 m. Better surface finish was obtained at smaller feed rates, and an optical quality surface of $0.026 \mu\text{m}$ in R_{\max} was achieved at a feed rate of $3 \mu\text{m}/\text{rev}$.^[12]

Synchronized two-direction vibration was applied to the cutting edge in the plane, including the cutting direction and the chip flow direction in such a way that the cutting edge formed an elliptical locus in each cycle of the vibration. This “elliptical vibration cutting” was effective to reduce the chip thickness and the cutting force, compared with the conventional cutting, including cutting with vibration. The shear angle was much increased when the frequency of the elliptical vibration was increased, and exceeded 60° at a frequency of 6 Hz.^[13]

Ultrasonic vibration was also used in grinding processes.^[14–17] Vibration-assisted grinding was examined,^[18,19] and the results showed that surface roughness was improved and grinding forces decreased. Low-frequency vibration (30 Hz) was introduced to the workpiece during creep feed grinding.^[20] The vibration amplitude was in the range of 0 to 1.5 mm. The risk of surface burning and tempering was reduced with increased vibration amplitude. Vibration with a frequency up to 400 Hz was used and grinding of a hardened nickel alloy was carried out, resulting in reduced cracking and surface burning.^[21] A superposition of grinding kinematics



with an axial tool oscillation in the ultrasonic range led to a significant increase in the material removal rate.^[13,22–24]

This study covers design, fabrication, and testing of a microvibration device. The study also covers establishment of the relationships of the driving voltage, vibration frequency, and displacement of the device. A comparison of ground surface quality under different grinding conditions (without vibration, with microvibration in the vertical, along or across the table-feed direction) is also included in the scope.

2. DESIGN OF A MICROVIBRATION DEVICE

Figure 1 shows the microvibration device designed. It consists of two mechanical systems to provide microvibration in the vertical and horizontal directions. The vertical vibration system has a sample plate and a sample base plate driven by three piezoelectric actuators. The horizontal vibration system has a moving platform driven by one piezoelectric actuator. The moving platform is fixed on the movable blocks of three linear motion guides and can vibrate horizontally.

Fast response is one of the desirable features of piezoelectric actuators. Minimum rise time of a piezoelectric actuator requires a power amplifier with sufficient output current. A piezoelectric ceramic material can withstand pressures up to a few hundred MPa before it breaks mechanically. Tensile loads on nonpreloaded piezoelectric ceramic materials are limited to 5 to 10% of the maximum compressive force. Preloaded elements are highly recommended for dynamic applications. When operated well below the resonant frequency, a piezoelectric actuator behaves as a capacitor (displacement is proportional to charge). In dynamic applications, the power consumption increases linearly with frequency and actuator capacitance.^[25]

Multilayer piezoelectric actuators were chosen to be used in the device because they have many advantages^[26]: low power consumption, high energy-conversion

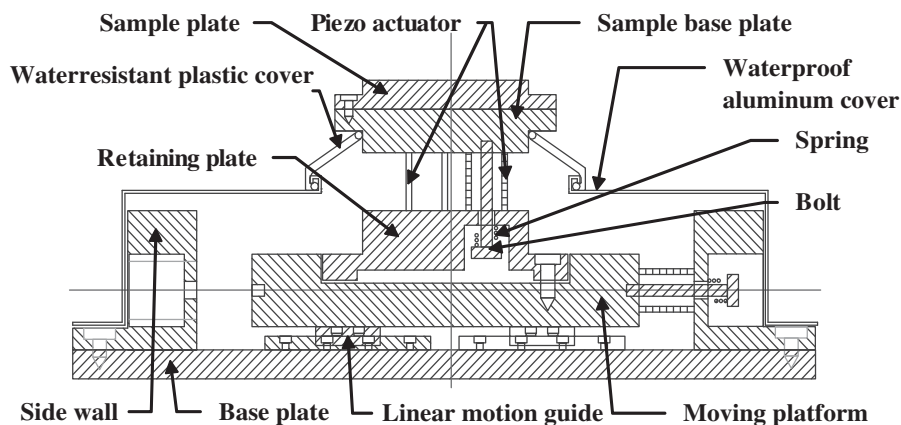


Figure 1. The microvibration device designed.

efficiency, large generated force, stable displacement, reduced shift and creep phenomena, high response speed, low drive voltage, ease of use, and low cost. The actuators selected have a resonance frequency of 69 kHz. They are driven by the output driving voltage of a power amplifier that amplifies the small sinusoidal input signal from a function generator.

Piezoelectric actuators are preloaded by springs and bolts. Piezoelectric ceramics must be protected from humidity or fluid contamination. Therefore, an aluminum waterproof cover and a plastic water-resistant cover are used to prevent coolant from flowing into the device for keeping the piezoelectric actuators in a dry working environment.

Three piezoelectric actuators are used to drive the sample plate and the sample base plate to move them along the vertical axis. Three sets of piezoelectric actuator, bolt, and spring are placed around the center of a retaining plate, which supports the piezoelectric actuators, the sample plate, and the sample base plate.

The whole vertical mechanism is fixed on the moving platform to obtain horizontal microvibration. Three linear motion guides support the moving platform and the whole vertical mechanism. One piezoelectric actuator is fixed between the moving platform and the side wall, along the central axis of the horizontal moving platform, to drive the movable parts. Three linear motion guides are placed at the vertexes of an isosceles triangle. The rails of the linear motion guides are aligned parallel to the horizontal axis, and the whole setting ensures the platform moving along the axis by constraining movements in other directions.

The whole device is made of aluminum except the base plate which is made of cast iron. The base plate can be attracted and mounted on the magnetic table of a grinding machine by its electromagnetic force.

The total available displacement can be calculated using the following equation^[25]:

$$\Delta L \approx \Delta L_0 \left(\frac{k_T}{k_T + k_S} \right) \tag{1}$$

where ΔL is displacement with external spring load (m), ΔL_0 is nominal displacement without external force or restraint (m), k_S is spring stiffness (N/m), and k_T is piezoelectric actuator stiffness. From Eq. (1), Eq. (2) is obtained for calculating k_S .

$$k_S \approx \frac{k_T}{\Delta L} (\Delta L_0 - \Delta L) \tag{2}$$

As $\Delta L_0 = 12.3 \mu\text{m}$, $k_T = 190.2 \text{ N}/\mu\text{m}$ for the piezoelectric actuator selected, the required spring stiffness can be calculated using Eq. (2) for certain total available displacement. Table 1 lists different maximum displacement values of the vibration device and the required spring stiffness.

However, the total available displacement can be achieved by choosing a spring with appropriate stiffness K_S . If a spring with stiffness of $0.1 K_T$ is selected, the total available displacement for horizontal vibration driven by one actuator with one spring is $11 \mu\text{m}$. Similarly, the total available displacement for vertical vibration

Table 1. Spring stiffness and maximum displacement of the vibration device.

ΔL (μm)	2	3	4	5	6	7	8	9	10	11	12
k_S (N/ μm)	980	590	395	278	200	144	102	70	44	22	5

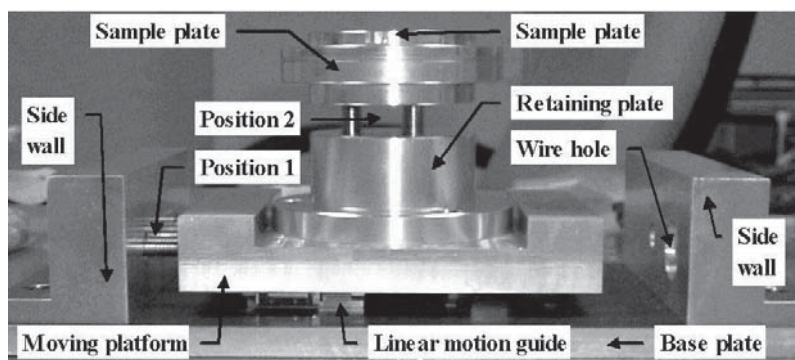


Figure 2. Front view of the microvibration device fabricated.

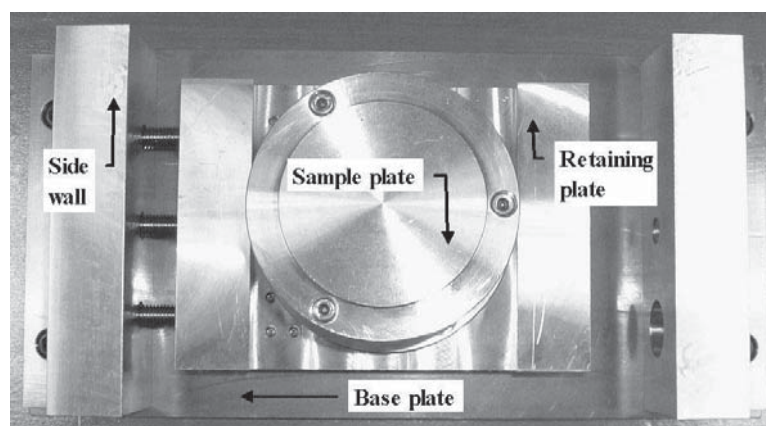


Figure 3. Top view of the microvibration device fabricated.

driven by one actuator with three springs can be calculated to be $9.5\ \mu\text{m}$. If the applied sinusoidal voltage varies between 0 and 100 V, the vibration displacement varies between 0 and $11\ \mu\text{m}$ for horizontal vibration and 0 and $9.5\ \mu\text{m}$ for vertical vibration. The maximum vibration displacement will decrease a little with loads.

3. EXPERIMENTAL RESULTS AND DISCUSSION

Figures 2 and 3 show two photographs of the microvibration device fabricated. The piezoelectric actuators, the aluminum waterproof cover, and the

plastic water-resistant cover are removed to show the inside structure. The whole device is covered by the water-resistant cover and water-resistant plastics during grinding.

The original design was that one piezoelectric actuator was installed at position 1, while the other three piezoelectric actuators were installed at position 2 along with the three bolts. However, due to the capacitive loading limit of the power amplifier used, only one piezoelectric actuator could be driven at one time by one power amplifier. Therefore, for the experiments, one piezoelectric actuator was installed at the center of the retaining plate to generate the vertical microvibration. Because the vibration displacement was in micrometer order and the workpiece was fixed on the center of the sample plate surface, three bolts and three springs could balance the driving force to a certain extent.

The vibration displacement was measured using an accelerometer. A charge amplifier was used to amplify the output signal of the accelerometer for monitoring. An oscilloscope was used for monitoring the driving voltage signal and the output signal from a function generator in the time domain. A dynamic signal analyzer was used for monitoring the driving voltage signal and the vibration displacement signal from the charge amplifier in the frequency domain. The relationships of the vibration displacement, driving voltage amplitude, and frequency were measured for the vertical and horizontal vibration systems.

The maximum operating frequency, f_{\max} , of the driving power amplifier used can be calculated using Eq. (3)^[25]:

$$f_{\max} \approx \frac{i_{\max}}{\pi C V_{p-p}} \quad (3)$$

where i_{\max} is peak amplifier source/sink current (A), C is piezoelectric actuator capacitance (F), and V_{p-p} is peak-to-peak driving voltage (V). When $i_{\max} = 0.1$ A, $V_{p-p} = 86.6$ V, and $C = 5.4$ μ F, the maximum operating frequency is 68 Hz.

Figure 4 shows that when the frequency was higher than 68 Hz, the driving voltage (output of the driving power amplifier) V_{p-p} dropped down, which caused the vertical vibration displacement to drop significantly. The system was stable when the driving frequency was between 18 and 68 Hz. This range was much smaller than the theoretically calculated range because of the restriction of the capacity-loading ability of the power amplifier used.

The driving voltage was increased continuously while the driving frequency was kept at 40 Hz, and the vibration displacement was recorded. The results are plotted in Fig. 5. The vibration displacement is proportional to the driving voltage V_{p-p} as shown by the chart. The relationship can be presented as $y = 0.0966x - 0.0559$, where y is vibration displacement (μ m) and x is driving voltage V_{p-p} (V). The maximum displacement is 9.4 μ m, which is approximately equal to the value (9.5 μ m) theoretically calculated using Eq. (1).

Figure 6 illustrates measurement results of horizontal direction vibration of the device. The maximum operating frequency calculated using Eq. (3) is 68 Hz. Figure 6 shows that the driving voltage V_{p-p} and the vibration displacement decrease with increasing vibration frequency when the frequency is higher than 68 Hz.

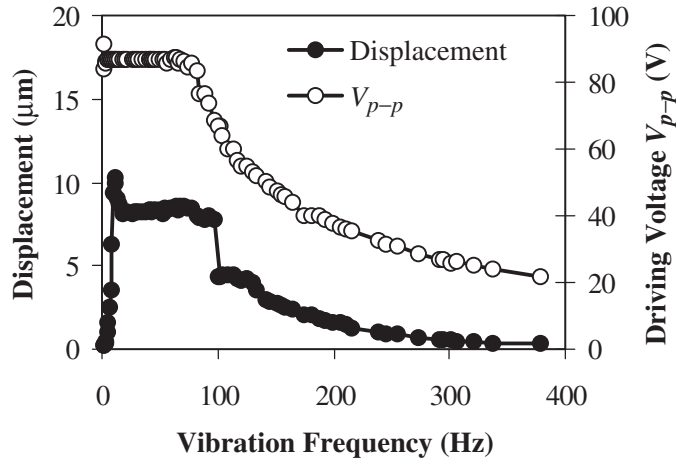


Figure 4. Vibration displacement and peak-to-peak driving voltage measured for vertical-direction motion.

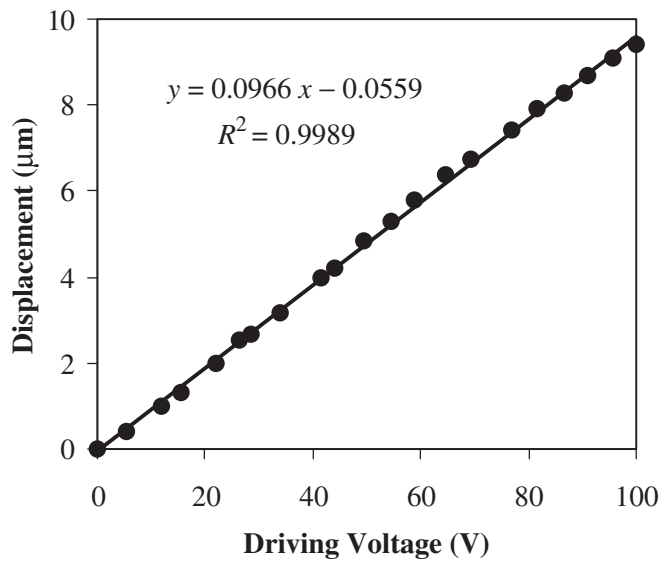


Figure 5. Vibration displacement vs. peak-to-peak driving voltage for vertical-direction motion.

The driving voltage was increased continuously while the driving frequency was kept at 80 Hz, and the horizontal vibration displacement was recorded. Figure 7 shows that the vibration displacement is proportional to the driving voltage V_{p-p} . The relationship can be presented as $y = 0.083x - 0.2398$, where y is vibration displacement (μm) and x is driving voltage V_{p-p} (V).

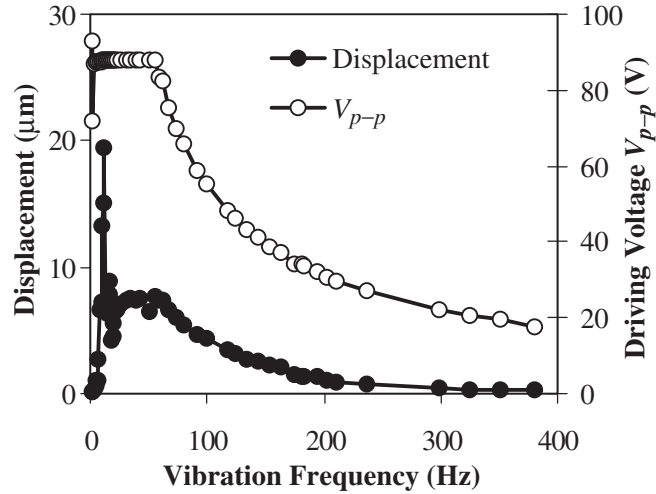


Figure 6. Vibration displacement and peak-to-peak driving voltage measured for horizontal direction motion.

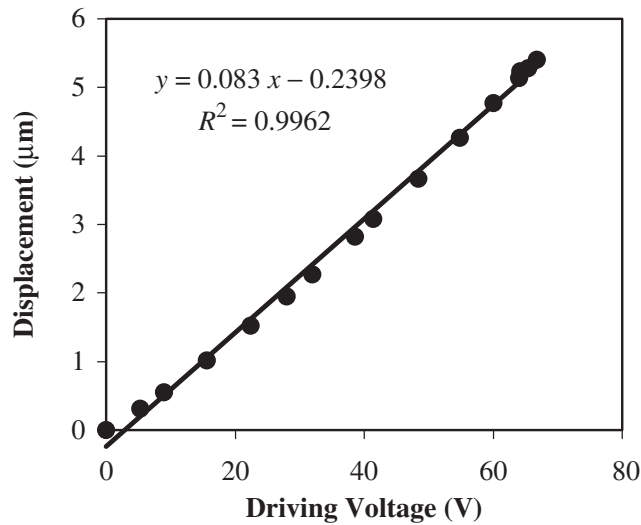


Figure 7. Vibration displacement versus peak-to-peak driving voltage for horizontal direction motion.

Four silicon samples were cut from the same wafer for grinding experiments without vibration (sample 1) and with microvibration in vertical (sample 2), table-feed (sample 3), and cross-feed (sample 4) directions. The samples were fixed on the center of the sample plate of the microvibration device using wax. The microvibration device was then mounted on the table of a surface grinding

Table 2. Grinding conditions.

Workpiece material	Silicon
Grind wheel	Resin bond diamond wheel, diameter = 355 mm, width = 10 mm
Wheel speed	27 m/s (1,450 rpm)
Cross feed	1 mm
Table speed	5 m/min

Table 3. Vibration parameters for grinding of the four samples.

Sample	1	2	3	4
Vibration direction	Without	Vertical	Table feed	Cross feed
Driving frequency (Hz)	0	114	80	66
Driving voltage V_{p-p} (V)	0	46.6	66.4	108
Vibration displacement (μm)	0	3.3	5	9.1

Table 4. Average values of the surface roughness heights.

Sample	R_a		R_q		R_t		R_z	
	μm	%	μm	%	μm	%	μm	%
1	0.098	100	0.126	100	0.801	100	0.630	100
2	0.047	48	0.060	48	0.382	48	0.324	51
3	0.051	52	0.067	53	0.535	67	0.383	61
4	0.046	47	0.057	45	0.365	46	0.312	50

machine. The grinding conditions are listed in Table 2. The vibration parameters for grinding of the four samples are shown in Table 3.

The grinding procedures were the same for the four experiments:

1. Truing and dressing of the diamond grinding wheel.
2. Grinding of 10 μm by 1 μm of down feed.
3. Grinding of 5 μm by 0.5 μm of down feed.
4. Grinding of 2 μm by 0.2 μm of down feed.

A precision surface roughness tester was used to measure the surface roughness of the ground samples. Each sample was measured five times along the cross-feed direction. Table 4 and Figs. 8 and 9 show the average values of the surface roughness heights for comparison. The surface roughness of the silicon sample ground with microvibration in the cross-feed direction was the best, with 45 to 50% of the roughness heights of the sample ground without vibration. The roughness of the sample ground with microvibration in the vertical direction was the next best.



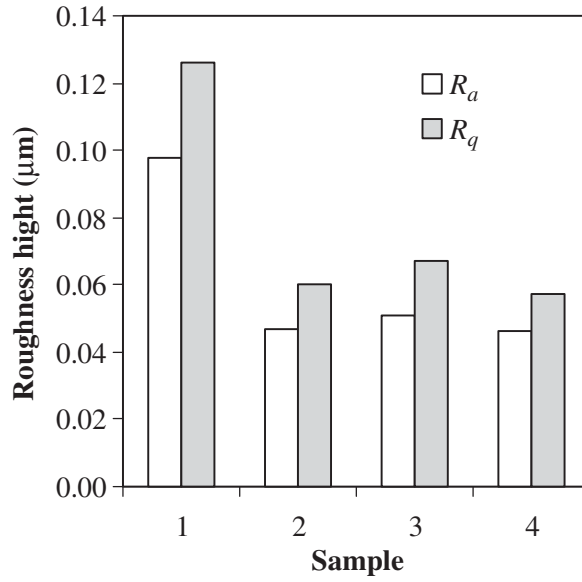


Figure 8. Surface roughness R_a and R_q of the ground silicon samples.

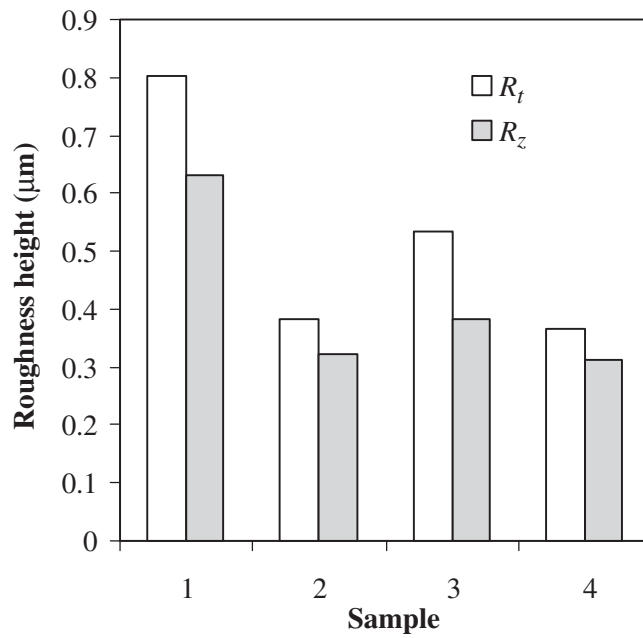


Figure 9. Surface roughness R_t and R_z of the ground silicon samples.



The surface roughness heights of the sample ground with microvibration in the table-feed direction were 33 to 48% better than those of the sample ground without vibration. This result is in line with what we have estimated: microvibration of the workpiece along a certain direction during grinding can improve the surface finish of the ground workpiece.

4. CONCLUSION

A microvibration device with adjustable vibration frequency and displacement was designed and fabricated to facilitate grinding experiments for analyzing the effect of workpiece microvibration on workpiece surface finish. The device can provide microvibration in vertical and horizontal directions. The relationships of the driving voltage, vibration displacement, and frequency were established. Grinding experiments were carried out to test the functions of the microvibration device and compare surface roughness of silicon samples ground with and without vibration. The results verified that microvibration of the workpiece along a certain direction during grinding can affect the surface finish of the ground workpiece. Further detailed research and improvement, such as increase of the stiffness of the device and more grinding experiments using a better power amplifier, will be carried out.

REFERENCES

1. Hegeman, J.B.J.W. Fundamentals of Grinding, Surface Conditions of Grind Materials, University of Groningen, Holland, 2000. <http://www.ub.rug.nl/eldoc/dis/science/j.b.j.w.hegeman/c2.pdf> (visited on 1 Jun 2003).
2. Zhong, Z.W. Partial-ductile grinding, lapping, and polishing of aspheric and spherical surfaces on glass. *Mater. Manuf. Proc.* **1997**, *12* (6), 1063–1073.
3. Zhong, Z.W. Machining of glass molds for manufacturing plastic lenses. *Mater. Manuf. Proc.* **2000**, *15* (3), 449–464.
4. Zhong, Z.W.; Hung, N.P. Diamond turning and grinding of aluminum-based metal matrix composites. *Mater. Manuf. Proc.* **2000**, *15* (6), 853–865.
5. Zhong, Z.W.; Ramesh, K.; Yeo, S.H. Grinding of nickel-based super-alloys and advanced ceramics. *Mater. Manuf. Proc.* **2001**, *16* (2), 195–207.
6. Malkin, S. *Grinding Technology, Theory and Applications of Machining with Abrasives*; Ellis Horwood Ltd: Dearborn, Michigan, USA, 1989.
7. Zhong, Z.W. Grinding of toroidal and cylindrical surfaces on sic using diamond grinding wheels. *Mater. Manuf. Proc.* **1997**, *12* (6), 1049–1062.
8. Zhong, Z.W. Ductile or partial ductile mode machining of brittle materials. *Int. J. Adv. Manuf. Technol.* **2003**, *21* (8), 579–585.
9. Zhong, Z.W.; Lee, W.Y. Grinding of silicon and glass using a new dressing device and an improved coolant system. *Mater. Manuf. Proc.* **2001**, *16* (4), 471–482.
10. Zhong, Z.W.; Tok, W.H. Grinding of single-crystal silicon along crystallographic directions. *Mater. Manuf. Proc.* **2003**, *18* (5), 811–824.





11. Moriwaki, T.; Shamoto, E.; Inoue, K. Ultraprecision ductile cutting of glass by applying ultrasonic vibration. *Ann. CIRP* **1992**, *41* (1), 141–144.
12. Moriwaki, T.; Shamoto, E. Ultraprecision diamond turning of stainless steel by applying ultrasonic vibration. *Ann. CIRP* **1991**, *40* (1), 559–562.
13. Shamoto, E.; Moriwaki, T. Study on elliptical vibration cutting. *Ann. CIRP* **1994**, *42* (1), 35–38.
14. Suzuki, K.; Tochinai, H. A new grinding method for ceramics using a biaxially vibrated non-rotational ultrasonic tool. *Ann. CIRP* **1984**, *39* (1), 329–332.
15. Nakagawa, T.; Suzuki, K.; Uematsu, T. Highly efficient grinding of ceramic and hard metals on grinding center. *Ann. CIRP* **1986**, *35* (1), 205–210.
16. Spur, G.; Holl, S.-E. Ultrasonic assisted grinding of ceramics. *J. Mater. Proc. Technol.* **1996**, *62* (1), 287–293.
17. Spur, G.; Holl, S.-E. Material removal mechanisms during ultrasonic assisted grinding. *Prod. Eng.* **1997**, *4* (2), 9–14.
18. Wang, Y.; Moon, K.S.; Miller, M.H. *Micro-Actuation in Precision Grinding*, Proceedings of the ASME Dynamics Systems and Control Division, 1996, Vol. 58, 349–356.
19. Wang, Y.; Moon, K.S.; Miller, M.H. A new method for improving the surface grinding process. *Int. J. Manuf. Sci. Prod.* **1998**, *3* (1), 159–167.
20. Hanasaki, S.; Fujivara, J.; Wada, T.; Hasegawa, Y. Vibratory creep feed grinding. *Trans. Japan Soc. Mech. Eng.* **1994**, *60* (573), 1829–1834.
21. Poletav, V.A.; Khrul'kov, V.A. Intermittent grinding with oscillation of the work. *Stanki Instrument* **1990**, *61* (1), 33–34.
22. Markov, A.I. Ultrasonic drilling of hard non-metallic materials with diamond tools. *Stanki Instrument* **1977**, *48* (2), 33–35.
23. Pei, Z.J. *Rotary Ultrasonic Machining of Ceramics, Characterization and Extensions*. M.S. thesis, University of Illinois, USA, 1995.
24. Uhlmann, E.; Holl, S.-E.; Daus, N.-A. Ultrasonic assisted grinding—part I. *Abrasives Magazine* **2000**, 8–14.
25. PI-Polyte Group, Tutorial, Piezoelectrics in Positioning Contents. <http://www.physikinstrumente.de/products/section4/content.php> (visited on 15 May 2003).
26. NEC-TOKIN, Multilayer Piezoelectric Actuators. <http://www.nec-tokin.com/now/english/product/pdf-dl/multilayerpiezoelectricActu.pdf> (visited on 15 May 2003).

Received September 19, 2003

Accepted December 4, 2003

